Bound-state dipole strength in ^{56}Fe

T. Chapuran,* R. Starr,† R. Vodhanel,‡ and M. K. Brussel
Department of Physics, University of Illinois at Urbana-Champaign, Urbana, Illinois 61801
(Received 3 February 1984)

Resonant photon scattering from ^{56}Fe has been measured from 5 to 10 MeV using Ge(Li) detectors and bremsstrahlung beams with end-point energies of 7.6 and 10.3 MeV. Energies and values of $g\Gamma_0^2/\Gamma$ were obtained for more than 40 levels, most of which have not been observed in previous photon experiments. Spins of 13 levels were determined from angular distribution measurements. In complementary lower-resolution ($\Delta E \sim 100$ keV) tagged photon measurements, average elastic and inelastic (to the first excited state) photon scattering cross sections were measured from 5.8 to 11.5 MeV (i.e., to above the neutron threshold). The combination of these measurements provides the most detailed account of bound-state dipole strength available in this mass region.

I. INTRODUCTION

The f-p shell nuclei have attracted considerable interest in recent years because they comprise one of the most favorable regions for observing a collective spin-flip $M1$ giant resonance. In the independent particle model, both the proton and neutron $1f_{7/2}$ subshells are filled at ^{56}Ni ($N=Z=28$), while both $1f_{5/2}$ subshells are empty. The (unperturbed) energy gap between the spin-orbit pairs is about 8 MeV. Theoretical calculations have predicted substantial $M1$ strength in this energy region,[1,2] and a number of nuclei have been investigated experimentally. ^{56}Ni is itself unstable, and most experiments have focused on the other $N=28$ isotones ^{48}Ca, ^{50}Ti, ^{52}Cr, and ^{54}Fe, or on the heavier isotopes of iron or nickel. Photoneutron production,[3] polarized photon scattering,[4] back angle electron scattering,[5,6] and charge exchange reactions[7] have provided a picture of an $M1$ resonance strength severely quenched by ground-state correlations and possibly by non-nucleonic effects such as Δ-hole polarization.[6,8] The measurements are made difficult by the weakness of the resonance, and by the fragmentation of its strength amid dense backgrounds of $E1$ and $M2$ transitions.

Substantial concentrations of $E1$ strength are, in fact, expected in the same energy region.[9] The distribution of the strength is ultimately related to the microscopic structure of the giant dipole resonance (GDR), which peaks near 20 MeV of excitation in these nuclei. The GDR has been thoroughly investigated in this region, most recently with both elastic and inelastic photon scattering[10] ($E_\gamma \geq 14$ MeV) from ^{56}Fe and ^{60}Ni. In contrast, however, almost nothing is known about the distribution of $E1$ strength below the particle thresholds. The few discrete $E1$ transitions which are known are largely the by-products of attempts to identify the $M1$ strength with polarized photon scattering.

Resonant photon scattering is an effective method for mapping out the distribution of dipole strength among bound levels. Photons in this energy region excite only $E1$, $M1$, and, to a lesser extent, $E2$ transitions. The $E2$ transitions are easily identified through angular distribution measurements, while $M2$ transitions are not excited at all. The selectivity of the reaction combined with the high resolution available with Ge(Li) detectors allows measurements of model-independent decay widths for discrete levels up to the particle thresholds, even for nuclei several particles removed from closed shells. The major limitation of such experiments in the past was the lack of intense sources of bremsstrahlung photons with energies above 5 MeV. This problem has been overcome in recent years with the development of high duty-cycle electron accelerators, which have permitted photon scattering measurements to be made with a much higher accuracy and sensitivity than had earlier been practical.

This paper reports on resonant photon scattering from bound states in ^{56}Fe. There are several reasons why ^{56}Fe was chosen for study. First, due to the large number of available spin-flip transitions, this nucleus is expected to exhibit one of the strongest $M1$ resonances in the region. Since the isobaric analog state ($T=3$) lies above the neutron threshold, only states with isospin equal to that of the ground state ($T_0=2$) will be observed in photon scattering. While the $M1$ strength is split into isospin components $T_< = T_0$ and $T_> = T_0+1$, more than two-thirds of the strength should be concentrated into $T_<$ levels in this neutron-excess nucleus. Since the neutron threshold is rather high (11.2 MeV), most of the $M1$ strength should be accessible to photon scattering, while the isospin of any states observed is unambiguously known. Second, the $E1$ giant resonance has been extensively studied in ^{56}Fe, thus facilitating the interpretation of the electric dipole strength below the neutron threshold. Finally, as an experimental consideration, iron is the only element in this region which is approximately monoisotopic (>90%) in an even-even isotope.

When the present work was begun, no decay widths were published for any dipole states above 5 MeV in ^{56}Fe. Widths for the seven states most strongly excited have since been reported by Kumagai *et al.*, using a low duty-cycle bremsstrahlung beam.[11] Very recently one additional level in this region has been measured by Smith and Segeth, using resonance absorption and resonance fluorescence of monoenergetic photons produced in the ^{13}C(p,γ)^{14}N reaction.[12] With our beams from the 100%

duty-cycle MUSL-2 accelerator,[13] the decay widths of more than 40 individual levels from 3 to 10 MeV in excitation have been measured. In addition, the elastic and inelastic ($E_x = 847$ keV, $J^\pi = 2^+$) photon scattering cross sections were measured with an energy resolution of 50—150 keV from 5.8 to 11.5 MeV, using tagged photons. The tagged photon data include contributions from weak transitions not visible above the backgrounds of conventional resonance fluorescence experiments, while the higher resolution data provide a more detailed account of the distribution of strength among the strongest levels. The combination of these two measurements provides the most detailed account of bound-state dipole strength in this mass region, and should provide a foundation for the future polarized photon scattering or electron scattering measurements which are still needed to distinguish the $M1$ and $E1$ contributions from each other.

II. EXPERIMENTAL PROCEDURE

A. Resonance fluorescence measurements

The bremsstrahlung photons used in the high resolution measurements were produced by 100% duty cycle electron beams of 7.6 and 10.3 MeV from the University of Illinois MUSL-2 accelerator.[13] The experimental arrangement has previously been described in detail.[14] Briefly, the bremsstrahlung converter was a 75 mg/cm^2 gold foil followed by a 14.8 g/cm^2 carbon beam stop, mounted inside an insulated Faraday cup. Photons scattered by a 2.4 g/cm^2 target of natural iron (92% ^{56}Fe) were observed with a 55 cm^3 Ge(Li) detector at an angle of 127° relative to the incident beam. Additional data were taken at 90° with the 7.6 MeV beam. The scattered photon beam was hardened with absorbers of copper and lead. In this experiment, the stainless steel (ss) end cap of the Faraday cup (1.25 g/cm^2 of ss 304, 62% ^{56}Fe) acted as a resonant absorber in the incident photon beam. This effect was taken into account in extracting decay widths from the measured yields (see Sec. III), and amounted to a correction of $\lesssim 12\%$ for the strongest transitions.

The signals from the detector were sorted into an 8192 channel spectrum in an on-line PDP-15 computer. The average counting rate in the detector was normally about 30 000 counts per second, and fast-logic pileup rejection techniques were employed. Test pulses from a precision, thermally stabilized pulser were used for a determination of pileup losses and for digital gain stabilization. The energy resolution under these conditions was better than 7 keV FWHM at 7 MeV for data accumulated over a 24 h period.

From the resulting spectra, peak centroids and areas were extracted using the computer program[15] SAMPO. The centroids were converted to energies using a linear calibration based on five levels (from 2.125 to 8.920 MeV) strongly excited in photon scattering from ^{11}B. The scattering yields were converted to cross sections using an empirical determination of $N_{\rm inc}(E)\epsilon(E)$, the product of the incident photon intensity with the detector efficiency. This quantity was measured by observing the scattering from nineteen levels (in six different nuclei) whose nuclear level parameters are known. Details of these calibration procedures, and the photon intensity curves used for the 7.6 and 10.3 MeV end point energy beams, have been presented in an earlier publication.[14]

B. Average photon scattering cross sections

The bremsstrahlung photons used in these measurements were produced by passing 40% duty cycle electron beams from the University of Illinois MUSL-1 microtron[16] through a thin (20 keV) aluminum foil. Electrons which lost energy in creating bremsstrahlung photons were momentum analyzed in a magnetic spectrometer, and detected in coincidence with photons scattered from the target. The energies of the incident photons were determined with a resolution of 50—150 keV using a focal plane array of 12 plastic scintillators to detect the residual electrons. The photons were collimated, scattered from a 10 g/cm^2 target of natural iron, and detected at an angle of 135° relative to the incident beam by a NaI(Tl) crystal, 15.2 cm in diameter by 22.9 cm deep. The 12 scattered-photon spectra (corresponding to the incident photons associated with each electron counter) were accumulated simultaneously using an on-line PDP-15 computer. Chance coincidence spectra were also accumulated, and the "true" spectra were obtained by subtracting these from the observed coincidences. The tagged photon system has been described previously in more detail.[17]

Average photon scattering cross sections were measured from 5.8 to 11.5 MeV, using electron beam energies of 9.5, 12.5, and 15.5 MeV. At the beginning of each run the target was removed and the NaI(Tl) detector was placed directly in the bremsstrahlung beam. In this way, the incident photon flux and the response of the NaI(Tl) crystal to the tagged photons associated with each electron counter were determined. The resolution of the NaI(Tl) crystal was sufficiently good (about 8%) to allow resolution of the ground state from the first excited state in ^{56}Fe ($E_x = 847$ keV, $J^\pi = 2^+$). The yields to the ground state and first excited state were extracted by fitting the true spectra with the measured response functions. At energies where the best chi-squared fit to the data required no inelastic scattering, the 2^+ cross section was taken to be zero (see Ref. 17 for a detailed description of the fitting procedure).

III. RESONANCE FLUORESCENCE RESULTS

The number of scattered photons from a resonance at energy E_r detected at an angle θ relative to the beam axis is given by

$$N_{\rm det} = N_{\rm inc}(E_r)\epsilon(E_r)W(\theta)A'(g,\Gamma,\Gamma_0,\Delta/\Gamma)\,. \qquad (1)$$

In this formula, $N_{\rm inc}(E_r)$ is the number of incident photons per unit energy at the resonance energy E_r, $\epsilon(E_r)$ is the detection efficiency (including the solid angle factor), and $W(\theta)$ is the angular distribution function for the emitted radiation, which depends only on the spins of the ground state (J_0) and the excited state (J_e), and on the multipolarity of the transition. A' is an effective photon scattering cross section, which depends on the target

thickness, the nuclear level parameters Γ and Γ_0 (the total decay width and the partial width for decay to the ground state, respectively), the statistical factor

$$g=(2J_e+1)/(2J_0+1)\ ,$$

and the Doppler width Δ.

For each beam energy, the product $N_{\rm inc}(E)\epsilon(E)$ was measured as a function of E, relative to the integrated electron beam current, by scattering from a large number of levels whose nuclear parameters were known. The quantity A' was then determined for new levels by measurements of the scattering yield and angular distribution. For elastic scattering from a thin target, A' is directly proportional to $g\Gamma_0^2/\Gamma$. Even for the thick targets used in the present experiment, it is essentially this same combination of parameters which is determined by a measurement of A'. For each transition, the effects of Doppler broadening and of atomic and nuclear resonant absorption in the target were taken into account numerically as described in Ref. 14. Typically, these effects produced 10% corrections to the magnitudes of $g\Gamma_0^2/\Gamma$ calculated from the thin-target formula ($\lesssim$23% corrections for the strongest transitions). These processes also introduce a dependence of the scattering yield on the branching ratio Γ_0/Γ (since the resonant absorption depends on Γ_0 but not on Γ), but this is a small effect for the target thickness used in the present experiment. The thick-target corrections were calculated assuming $\Gamma_0/\Gamma=1$ for all levels; however, using $\Gamma_0/\Gamma=0.5$ would have affected our results by less than 10% even for the strongest transitions. In the present experiment it was also necessary to account for resonant absorption of the incident photon beam in the stainless steel (62% ^{56}Fe) end cap of the Faraday cup. This was done in an iterative procedure, using the formalism developed in Ref. 14 for the analysis of self-absorption data. Initial values of Γ_0 were obtained from the scattering measurements, neglecting the upstream absorber and setting $\Gamma_0/\Gamma=1$. For each level the resonant absorption was then calculated from Γ_0, giving a correction to the photon flux incident on the scattering target at that energy. Using this slightly reduced photon flux, a new value of A' was calculated, and a new value of Γ_0 was obtained. After two or three iterations, self-consistent solutions for Γ_0 were obtained. The final values typically differed from the initial results by a few percent, and by $\lesssim$12% for the strongest transitions (for which the effect is most important).

The experimental results from the resonance fluorescence experiments are summarized in Table I. Spins of 13 levels were determined from measurements at 90° and 127° using a 7.6 MeV electron beam. Values of Γ_0^2/Γ for 46 levels were extracted from the 127° data taken with 7.6 and 10.3 MeV beams. As noted in Table I, five of these levels appear to be unresolved multiplets, and two others are given tentative assignments because of insufficient statistics or resolution. A portion of the 7.6 MeV spectrum at 127° is shown in Fig. 1, to indicate the quality of the data. The overall sensitivity of the measurements can be gauged by the clean observation of the weak transitions at 5.227 and 7.066 MeV ($\Gamma_0^2/\Gamma=0.037$ and 0.11 eV, respectively). The spectrum taken with a 10.3 MeV beam is shown in Fig. 2, where only the more prominent peaks are labeled. A comparison of the overlapping energy region in Figs. 1 and 2 (from 5.8 to 7.6 MeV) demonstrates the marked improvement in peak-to-background ratios obtainable by choosing the photon end point energy just above the region of interest. The transition labeled 7.918 MeV in Fig. 2 is probably produced by neutron capture[18] on copper in the detector shielding. The higher energy portion of Fig. 2 shows the rapidly increasing complexity of the spectrum above 8 MeV as the level density increases.

The spins of 13 levels were determined from measurements at 90° and 127° with a 7.6 MeV beam. Table II gives the ratios of the cross sections at 90° and 127°; the predicted values for dipole and quadrupole scattering from a spin-zero nucleus are 0.73 and 2.20 (taking account of our finite angular acceptance). The listed uncertainties are statistical only. The 5.257 MeV transition is the only case consistent with quadrupole scattering, and this state must have $J^\pi=2^+$ (since photons do not readily excite $M2$ transitions). Twelve dipole transitions were also identified, including the previously known[19] $M1$ transition at 3.449 MeV, and the 6.926 and 7.211 MeV transitions previously assigned as dipoles by Kumagai *et al.*[11] The measured ratios for the 3.449 and 5.227 MeV transitions are somewhat higher than expected, possibly due to feeding of these levels from higher-lying states, as will be discussed below. The weighted average of the measured ratios for the remaining ten dipole transitions is 0.78 ± 0.04 (statistical errors only), in substantial agreement with the predicted value of 0.73. Measurements made for four additional transitions (at 5.404, 5.853, 6.078, and 6.219 MeV) showed angular distribution ratios intermediate between the elastic scattering pure dipole and quadrupole predictions. These transitions are most likely due to branching of known higher-lying states to the first excited state in ^{56}Fe, as will be discussed below.

The values of Γ_0^2/Γ listed in Table I were extracted from the 127° scattering measurements assuming dipole angular distributions for levels whose spins were not measured. (The strong transitions at 8.128, 8.239, and 8.536 MeV are also known to be dipole from the results of Ref. 11.) The listed uncertainties include both statistical errors and a 15% uncertainty in the absolute normalization for levels distant from the end point energy of the photon beam. (See Ref. 14 for a discussion of the calibration procedures and associated uncertainties.) Twenty of the levels listed in Table I were excited with both the 7.6 and 10.3 MeV beams. The values of Γ_0^2/Γ extracted from these two measurements generally were in good agreement, and were combined to produce the values listed in Table I. Several of the low-energy transitions (at 3.449, 3.602, 4.847, 5.227, and 5.853 MeV) and the tentative 7.283 MeV transition showed significantly higher yields with the 10.3 MeV beam, which indicates feeding from higher-lying levels. For these transitions, only the 7.6 MeV results were used. Of course, such effects are most likely to be serious for weakly excited levels far from the end point energy.

All of the widths listed in Table I were extracted assuming the photons were scattered from levels in ^{56}Fe.

TABLE I. Comparison of measured level widths for ^{56}Fe. Values of Γ_0^2/Γ were extracted from the present experiment assuming $J=1$ where not measured (except $J=2$ for the level at 3.602 MeV); quoted uncertainties include statistical and calibration errors. Parentheses indicate tentative assignments, while levels in curly braces are probably unresolved multiplets. All results were calculated assuming elastic scattering from ^{56}Fe. (See the text for discussion.)

Energy[a] (keV)	J^a	Γ_0^2/Γ[a] (eV)	Γ_0^2/Γ[b] (eV)	Γ (eV)
3448.8±1.5	1	0.077 ±0.012		$\Gamma>0.035$[c]
{3602 ±3}		0.011 ±0.002		$\Gamma=0.004\pm0.002$[d]
4847 ±3		0.0071±0.0030		
5227 ±2	1	0.037 ±0.006		
5257 ±3	2	0.023 ±0.004		
5404 ±3[e,f]		0.027 ±0.006		
5853 ±2[e]		0.024 ±0.006		
6078 ±3[e]		0.028 ±0.005		
6219 ±3[e]		0.034 ±0.008		
6250 ±3	1	0.056 ±0.013		
6698 ±3	1	0.044 ±0.010		
6926 ±2	1	0.70 ±0.11	1.10±0.29	
7066 ±3	1	0.11 ±0.02		
7135 ±3	1	0.056 ±0.010		
7167 ±3	1	0.089 ±0.015		
7211 ±2[g]	1	0.50 ±0.08	0.77±0.22	
7248 ±2	1	0.20 ±0.03		
(7283 ±3)		0.29 ±0.12		
7446 ±2	1	0.17 ±0.05		
7468 ±2	1	0.18 ±0.03		
7886 ±4		0.28 ±0.05		
{8128 ±2}		1.94 ±0.30	3.55±0.74	
8219 ±4		0.26 ±0.05		
8239 ±2		2.63 ±0.42	5.75±0.92	
8307 ±4[e,f]		0.24 ±0.08		
8536 ±2		2.04 ±0.31	4.92±0.95	
8767 ±3		0.41 ±0.08		
8879 ±4		0.30 ±0.08		
8908 ±4		0.47 ±0.10		
{8961 ±4}		0.38 ±0.07		
8989 ±4		0.31 ±0.07		
{9107 ±4}		0.86 ±0.18		
9138 ±4		0.57 ±0.12		$\Gamma_{\gamma 0}=1.28\pm0.17$[h]
9154 ±5		0.95 ±0.31		
9287 ±3		0.75 ±0.17		
9311 ±4		0.64 ±0.13		
9322 ±4		0.65 ±0.14		
9402 ±3		0.65 ±0.15		
9558 ±4		0.39 ±0.14		
(9666 ±5)		0.67 ±0.22		
{9737 ±5}		0.95 ±0.25		
9768 ±4[f]		0.48 ±0.13		
9895 ±5[f]		0.41 ±0.12		
9948 ±5		0.75 ±0.20		
9969 ±5[f]		0.31 ±0.10		
10060 ±5		0.56 ±0.16		

[a]This work.
[b]Reference 11.
[c]$t_{1/2}<13$ fs; Ref. 19.
[d]$t_{1/2}=0.12^{+7}_{-5}$ ps; Ref. 19.
[e]May be an inelastic transition; see the text and Table III.
[f]May include contribution from an unidentified level.
[g]Transition has no uncontaminated peak in the 10.3 MeV spectrum; the 6.698 MeV contribution was subtracted to obtain this result.
[h]Reference 12.

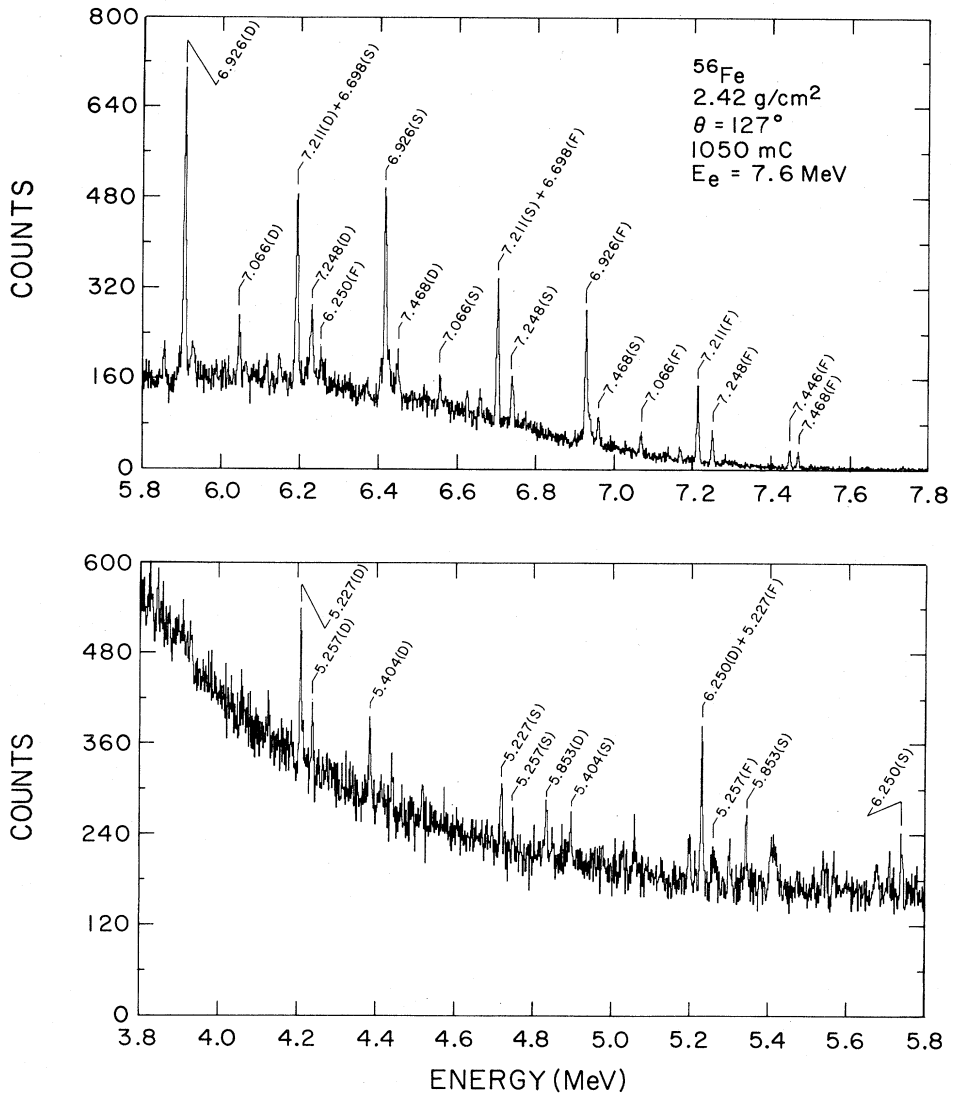

FIG. 1. Part of the spectrum obtained with 7.6 MeV end point energy bremsstrahlung scattered from a 2.42 g/cm^2 natural iron target (92% ^{56}Fe). The integrated beam current was 1050 mC. (*F*), (*S*), and (*D*) refer to the full energy, single- and double-escape peaks, respectively. One channel corresponds to 1.41 keV.

The natural iron target contained 92% ^{56}Fe, 6% ^{54}Fe, and 2% ^{57}Fe; the photoneutron thresholds for these isotopes are 11.20, 13.38, and 7.65 MeV, respectively. Given the low abundance and low neutron threshold of ^{57}Fe, even the strongest transitions in this nucleus should have been below our experimental sensitivity. We have not observed any of the known transitions[20] in ^{54}Fe, but it is possible that a few of the weakest transitions listed above 5 MeV might correspond to very strongly excited levels in ^{54}Fe. (A level in ^{54}Fe with $\Gamma_0^2/\Gamma = 3.1$ eV would be required to produce the same yield as a level in ^{56}Fe with $\Gamma_0^2/\Gamma = 0.2$ eV.)

All values of Γ_0^2/Γ were calculated assuming elastic scattering from levels with ground state branching ratios $\Gamma_0/\Gamma = 1$ (although, as mentioned above, the results would be only slightly different for other branching ratios, as long as $\Gamma_0/\Gamma \gtrsim 0.5$). Since all of the states observed are below the (γ,n) and (γ,p) thresholds, only electromagnetic decays are possible. The cross section for inelastic scattering (i.e., excitation of a resonance followed by photon decay to an excited state) is proportional to $\Gamma_0\Gamma_i/\Gamma$, where Γ_i/Γ is the branching ratio to the final (excited) state i. Direct observation of such branches is generally difficult in bremsstrahlung experiments because the inelastically scattered photons have lower energies, and significantly worse peak-to-background ratios than their elastically scattered counterparts. This also implies that the elastic scattering should be observable along with any inelastic scattering involving the same resonance, unless Γ_0/Γ is significantly less than 0.5.

Most of the transitions listed in Table I are unambiguously identified as resulting from elastic scattering due to energy considerations alone. All of the transitions above 5.6 MeV were excited within 2 MeV of the end point ener-

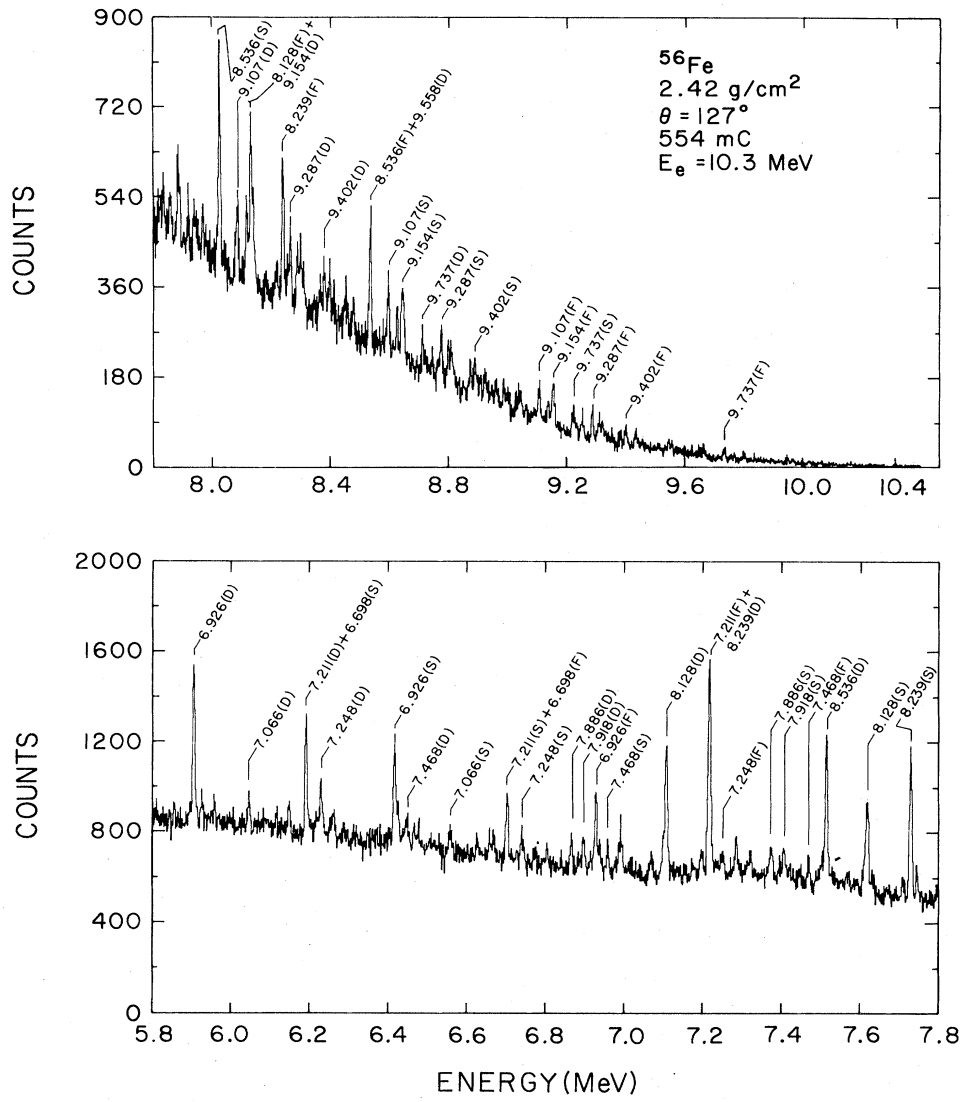

FIG. 2. Part of the spectrum obtained with 10.3 MeV end point energy bremsstrahlung scattered from a natural iron target. One channel corresponds to 1.36 keV.

gy of one of the bremsstrahlung beams (including a 9.5 MeV beam used in a preliminary run). Only the first excited state in ^{56}Fe ($E_x = 847$ keV, $J^\pi = 2^+$) lies below 2 MeV in excitation. In fact, 25 of the 40 transitions above 5.6 MeV were excited within 847 keV of one of the end point energies, and two more were only 50 keV farther away. (The photon flux 50 keV below the end point is sufficiently small to rule these out as well.) Two additional transitions at low energy are known to be elastic from other experiments. These considerations do not rule out an inelastic origin for the eight low-energy transitions between 4.8 and 6.3 MeV, the six transitions from 7.8 to 8.6 MeV (in the gap between the 7.6 and 9.5 MeV beams), or the three transitions at 8.767, 8.908, and 8.989 MeV, which were not cleanly observed with the 9.5 MeV beam (possibly due to relatively poor resolution and statistics).

A search was made for evidence of branching of the observed resonances to excited states, consistent with these constraints. Five of the possible inelastic transitions have energies corresponding to decay of higher-lying levels to the 847 keV 2^+ state; four of the five assumed parent resonances are known to be populated via elastic scattering. These cases are listed in Table III, along with the branching ratios extracted for the parent states assuming no other decay channels are significant, and assuming a dipole angular distribution. [Since $P_2(\cos\theta) \approx 0$ at 127°, this amounts to neglecting the P_4 term, whose coefficient is undetermined.] Since our data do not definitively identify these transitions as inelastic, they have also been analyzed as elastic resonances and included in Table I for completeness. However, as shown in Table II, the angular distribution ratios for the four transitions measured fall far from the predictions for pure dipole or quadrupole elastic scattering (whereas their assumed parent resonances are all in good agreement with the elastic dipole ratio). The yields for two additional transitions, at 5.227 and 6.250 MeV, could be augmented by branching of higher levels (at 7.886 and 8.908 MeV, respectively) to the 2^+ state at

TABLE II. ^{56}Fe angular distribution measurements. Listed uncertainties are statistical only.

Energy (MeV)	$W(90°)/W(127°)$	J
3.449	0.86±0.07	1
5.227	0.98±0.18	1
5.257	2.22±0.31	2
5.404[a,b]	1.21±0.29	
5.853[b]	1.56±0.31	
6.078[b]	1.35±0.33	
6.219[b]	1.30±0.28	
6.250	0.85±0.25	1
6.698	0.84±0.29	1
6.926	0.75±0.07	1
7.066	0.61±0.11	1
7.135	0.56±0.31	1
7.167	0.71±0.18	1
7.211	0.86±0.12	1
7.248	0.84±0.11	1
7.446	1.04±0.23	1
7.468	0.93±0.16	1

	$W(\theta)$	$W(90°)/W(127°)$
Dipole	$1+0.500P_2(\cos\theta)$	0.73
Quadrupole	$1+0.357P_2(\cos\theta)+1.143P_4(\cos\theta)$	2.28[c]

[a]Possible interference from unidentified levels.
[b]Possible inelastic transition; see the text and Table III.
[c]The experimental ratio is reduced to 2.20 by the finite angular acceptance of the detector.

2.658 MeV. The transition at 7.283 MeV could also be augmented by branching of the 8.128 MeV resonance to the first excited state. Since all three transitions were observed with the 7.6 MeV beam, they cannot arise entirely from these channels. The 5.227 and 7.283 MeV yields did increase significantly with the 10.3 MeV beam, and only the 7.6 MeV data were used in extracting the decay widths for these states. The 6.250 MeV yield, on the other hand, was very consistent for the two beam energies. None of the remaining inelastic candidates correspond in energy to branching of observed resonances, and therefore these transitions most likely arise from elastic scattering.

The decay widths extracted from the present experiment are compared with results of earlier measurements in Table I. Only one level below 5 MeV was strongly excited in our work, the known $M1$ transition at 3.449 MeV. Our result of $\Gamma_0^2/\Gamma=77\pm12$ meV, combined with the adopted branching ratio[21] $\Gamma_0/\Gamma=0.50\pm0.06$, yields $\Gamma=308\pm61$ meV, consistent with the lower limit of 35 meV extracted from Doppler shift attenuation lifetime measurements.[19] However, our spectra indicate that the branch to the first excited state (via the 2.602 MeV transition) is significantly weaker than the value $\Gamma_1/\Gamma=0.50\pm0.06$ reported in Ref. 21. Assuming no other decay channels are important, we obtain $\Gamma_0/\Gamma=0.79\pm0.02$, where the quoted error is purely statistical. This branching ratio leads to a value for the decay width $\Gamma=123\pm20$ meV. This should probably be interpreted as an upper limit, since the level is so far below the 7.6 MeV photon end point energy, and since the yield obtained with the 10.3 MeV beam was 50% larger, indicating the likelihood of substantial feeding from higher-lying levels. A much weaker transition was also observed at 3.602 MeV which appeared to be a doublet. The lifetime of one state at this energy ($J^\pi=2^+$) has been measured with the Doppler-shift attenuation method,[19] and accounts for only a small fraction ($\Gamma_0^2/\Gamma=1.7\pm0.8$ meV) of our observed strength if the branching ratio $\Gamma_0/\Gamma=0.65\pm0.10$ reported in Ref. 21 applies to this same level. In any case, our result for the combined strength of the doublet is itself an upper limit, as the yield with the 10.3 MeV beam was almost four times larger than with the 7.6 MeV beam, indicating very strong feeding from above. Obviously the properties of the states below 5 MeV could be much more appropriately investigated with lower end point energy beams. We report these results only for completeness, and to indicate the discrepancy with the previously published branching ratio.

Above 5 MeV in excitation, the previously available results are predominantly from the resonance fluorescence experiment of Kumagai *et al.*,[11] which utilized brems-

TABLE III. Possible branching in ^{56}Fe. See the text for discussion. The uncertainties include statistical errors and a 10% uncertainty in the relative detector efficiencies.

Energy (keV)	Branch	Γ_0/Γ
5404	6250(1)→847(2^+)	0.54±0.04
5853	6698(1)→847(2^+)	0.41±0.10
6078	6926(1)→847(2^+)	0.92±0.01
6219	7066(1)→847(2^+)	0.63±0.04
8307	9154 →847(2^+)	0.71±0.08

strahlung produced by a 14 MeV betatron beam. Widths were reported in Ref. 11 for the seven most strongly excited levels above 5 MeV, including dipole states at 10.479 and 11.133 MeV ($\Gamma_0^2/\Gamma=3.44$ and 2.08 eV, respectively[11]) which were beyond the energy range of the present experiment. Table I shows a systematic disagreement between the two measurements of the strengths for the five remaining transitions. The strengths reported by Kumagai *et al.* are about 55% higher than the present measurements indicated for the two levels near 7 MeV (6.926 and 7.211 MeV), and are on the average more than 100% higher for the three transitions near 8 MeV (8.128, 8.239, and 8.536 MeV). The pattern suggests a serious discrepancy in the calibration of the incident photon intensity over this energy region. In both experiments, this quantity was calibrated by scattering from levels whose widths were known; however, our procedure (Ref. 14) used many more states (nineteen rather than six) in a greater variety of nuclei (six rather than two) than were investigated in Ref. 11. In addition, the energy dependence of the yield was measured for six different end point energies in Ref. 14, which allowed a much more accurate determination of the shape of these curves than can be extracted from measurements with a single beam energy. An important check on the absolute normalization of the two experiments is provided by the tagged photon measurements discussed in Sec. IV, in which the product of the incident photon intensity and the detector efficiency was measured directly with the detector placed in the incident beam. These low resolution (~ 100 keV) coincidence measurements place upper limits on the widths of individual levels, since the measured yields include contributions from many weak levels not individually resolvable above the backgrounds of the high-resolution experiments. However, the width reported by Kumagai *et al.* for the line at 8.536 MeV ($\Gamma_0^2/\Gamma=4.92\pm0.95$ eV) is 45% larger than the total photon strength observed with tagged photons ($\Gamma_0^2/\Gamma=3.40\pm0.45$ eV) over a 100 keV interval about this energy. The present experiment indicates that only about 60% of this total strength ($\Gamma_0^2/\Gamma=2.04\pm0.31$ eV) is contained in the transition at 8.536 MeV.

Recently, Smith and Segeth[12] have reported a 1^- level at 9139.5 ± 0.6 keV with a width $\Gamma_{\gamma 0}=1.28\pm0.17$ eV (assuming $\Gamma_0/\Gamma=1$), based on resonance absorption and resonance fluorescence using NaI detectors and a monoenergetic source of photons (produced by proton capture). While we do observe a transition at 9138 ± 4 keV, our measurement gives a value $\Gamma_0^2/\Gamma=0.57\pm0.12$. There is no evidence of branching in our spectrum, and although the elastic peaks are not completely resolved from the neighboring 9154 keV transition, errors in extracting the areas could not account for the size of the discrepancy. It should be noted that similar previous experiments by the two groups on levels in ^{208}Pb near 5 and 7 MeV (Refs. 14 and 24) have shown excellent agreement, and the cause of the present discrepancy is not understood.

From the results in Table I it is clear that the sensitivity of the present experiment was more than an order of magnitude higher than the previous bremsstrahlung experiment reported in Ref. 11. This was partly due to the lower backgrounds obtainable with our lower end point energy beams (7.6 and 10.3 MeV as opposed to 14 MeV), and partly due to better statistics. The high average currents available from our machine (up to 20 μA) also allowed the use of a relatively thin target (2.4 g/cm^2 as opposed to 13.6 g/cm^2 in Ref. 11), which minimized the absorption corrections for the strong transitions, and the resultant dependence of the scattering yields on Γ_0/Γ. The spectrum presented in Ref. 11 was collected over a period of more than 800 h; the spectra shown in Figs. 1 and 2 were obtained in runs of 30 and 20 h, respectively, with our 100% duty-cycle accelerator.

IV. AVERAGE PHOTON SCATTERING CROSS SECTIONS

The quantity directly measured in the tagged photon experiment is N_t/N_γ, the ratio of the number of scattered photons detected at 135° to the number of incident photons of energy E_γ, averaged over the resolution ΔE. This ratio is related to the photon scattering differential cross section at 135° through the equation:

$$\frac{N_t}{N_\gamma}=\frac{1}{G}\frac{1}{\Delta E}\times\int_{\Delta E}\frac{d\sigma}{d\Omega}\bigg|_{135^\circ}\left\{\frac{1-\exp[-(2\sigma_e+\beta\sigma_a)n]}{2\sigma_e+\beta\sigma_a}\right\}dE\ . \tag{2}$$

In this equation, G is a geometrical factor involving the solid angle of the collimated detector. The quantity within the curly braces is an effective target thickness, which includes the effects of atomic and nuclear photon absorption in the target (with cross sections σ_e and σ_a, respectively). The quantity n is the target thickness per unit area perpendicular to the beam, and β is the fractional abundance of the isotope responsible for the nuclear absorption.

In energy regions where the level density is high, one can assume that nuclear self-absorption is negligible because the linewidths of the individual levels contributing to nuclear scattering are small. If one then defines the atomic absorption correction as

$$A=\frac{2\sigma_e}{1-e^{-2\sigma_e n}}\ , \tag{3}$$

and if the atomic absorption σ_e does not vary strongly over the energy interval ΔE, then Eq. (2) yields an expression for the energy-averaged differential cross section in terms of measured quantities:

$$\overline{\frac{d\sigma}{d\Omega}}\bigg|_{135^\circ}\equiv\frac{1}{\Delta E}\int_{\Delta E}\frac{d\sigma}{d\Omega}\bigg|_{135^\circ}dE=\frac{N_t}{N_\gamma}GA\ . \tag{4}$$

The further assumption that only dipole transitions contribute makes it possible to infer the average total elastic cross section $\overline{\sigma_{\gamma\gamma}}$ from these results:

$$\overline{\sigma_{\gamma\gamma}}=\left[\frac{N_t}{N_\gamma}\right]SGA\ , \tag{5}$$

where

$$S=\overline{\sigma_{\gamma\gamma}}\Big/\left.\frac{\overline{d\sigma}}{d\Omega}\right|_{135^\circ}=11.17\ \text{(dipole)}\ . \tag{6}$$

When individual nuclear levels can be resolved, it is possible to correct for nuclear self-absorption[17] by writing the cross section σ_a in terms of the Doppler-broadened line shape,[22] and numerically evaluating the integral in Eq. (2) for assumed values of the nuclear parameters g, Γ, Γ_0, and Δ/Γ (where Δ is the Doppler width). As discussed in Sec. III, the elastic scattering measurement then determines the product $g\Gamma_0^2/\Gamma$. If the average cross section data contain contributions from several unresolved, strongly excited levels, the proper self-absorption corrections can be made only if the widths of the strong levels are known from higher resolution measurements.

The average elastic differential cross section at 135° for natural Fe is displayed graphically in Fig. 3. Also shown is the 135° differential cross section for scattering to the first excited state in ^{56}Fe at 847 keV. Natural Fe contains 92% ^{56}Fe, 6% ^{54}Fe, and 2% ^{57}Fe. Scattering from ^{57}Fe is a small fraction of the total due to the low abundance, and above the neutron threshold at 7.6 MeV this isotope should not contribute at all. The cross sections drop close to zero above 11.2 MeV, where only the small contribution from ^{54}Fe remains. Therefore, the top part of Fig. 3 may be considered a good representation of the ^{56}Fe elastic scattering cross section.

The results presented in Fig. 3 do not include corrections for nuclear self-absorption. Neglecting this correction is valid where the individual contributing levels have widths that are less than a few tenths of an eV. Examination of the higher resolution resonance fluorescence results presented in Sec. III indicates that this is the case over most of the energy region covered in the tagged photon experiment. Where there are strong levels, however, the data displayed in Fig. 3 underestimate the scattering cross sections. The error bars on the data points reflect statistical uncertainties only. Systematic errors are estimated to be no larger than 8%, arising from uncertainties in the photon flux (±5%), G (±5%), A (±3%), and the photon energy E (±1%).

The elastic scattering cross section shown in Fig. 3 exhibits pronounced structure as a function of photon energy. Only a few of the structures, all below 9 MeV, are predominantly due to individual strongly excited levels, and only a fraction of the total strength can be accounted for by the discrete lines reported in Sec. III. (See Sec. V for a detailed comparison of the low- and high-resolution measurements.) It is interesting to note that the inelastic scattering cross section is generally less than half as large as the elastic strength. A comparable ratio of inelastic to elastic scattering has been observed in the giant dipole region (14—22 MeV) by Bowles *et al.*[10] Their results were interpreted as reflecting the effects of coupling between the dipole resonance and collective surface vibrations (as predicted, e.g., by the dynamic collective model[23]). For individual bound levels, the inelastic (elastic) scattering yield is proportional to Γ_i/Γ (Γ_0/Γ); thus the ground state branching ratios must typically be $\gtrsim 0.7$. There is also very little correlation between the elastic and inelastic excitation functions except in the region above 10 MeV.

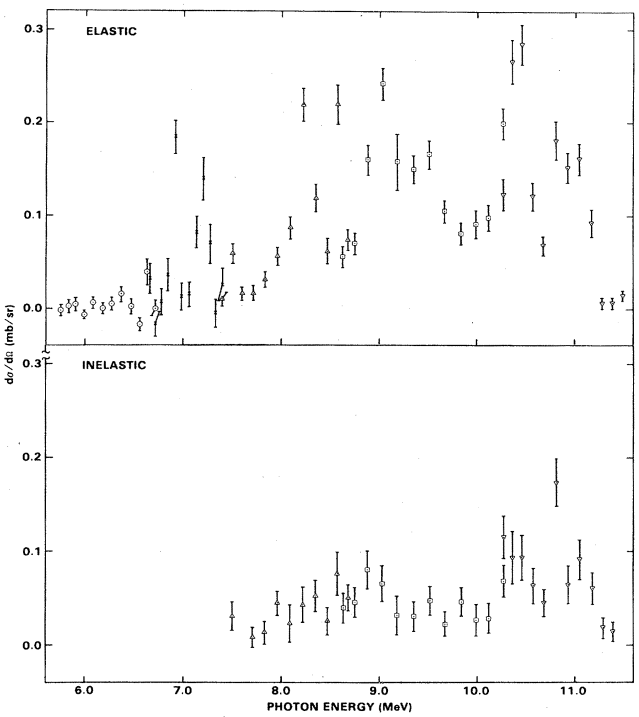

FIG. 3. Average 135° differential cross section for elastic photon scattering from natural iron, and for inelastic photon scattering leaving ^{56}Fe in its first excited state ($E_x=847$ keV, $J^\pi=2^+$). The different symbols plotted correspond to data taken with five different field settings in the electron spectrometer. No corrections have been made for nuclear absorption in the target.

Of course, the discrete lines which dominate the scattering in several of the lower energy regions are known not to have strong branches to excited final states (see Sec. III).

The total photon absorption cross section $\sigma_{\gamma T}$ can be extracted from the present work under the assumptions that the scattering is dominated by dipole excitations (as expected from consideration of the $E1$, $M1$, and $E2$ sum rules), and that inelastic scattering to more highly excited states can be neglected. The differential cross sections were converted to total cross sections according to Eq. (6), with $S=11.17$ for the elastic dipole scattering and $S=12.41$ for the (nearly isotropic) inelastic scattering to the first excited state. These two cross sections were then added to obtain $\sigma_{\gamma T}$. The results are shown in Fig. 4, along with an extrapolation to these energies of the giant dipole resonance in ^{56}Fe, using the Lorentz parameters listed in Table IV and obtained from the photon scattering measurements of Bowles *et al.*[10]

V. DISCUSSION AND CONCLUSIONS

The relationship between the resonance fluorescence decay widths (Sec. III) and the average photon scattering cross sections (Sec. IV) is most easily seen for the case of a single isolated level. The integral of the elastic scattering

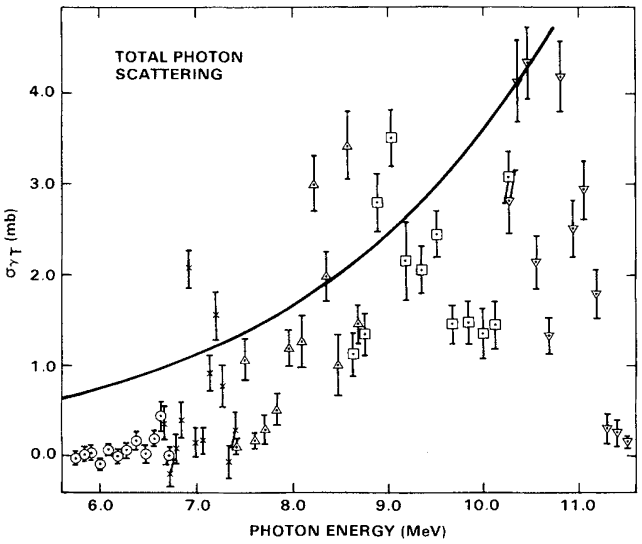

FIG. 4. Total photon absorption cross section for ^{56}Fe, obtained from the measured elastic and inelastic differential cross sections (see the text for discussion). The solid curve is a low energy extrapolation of the Lorentz lines which fit the giant dipole resonance.

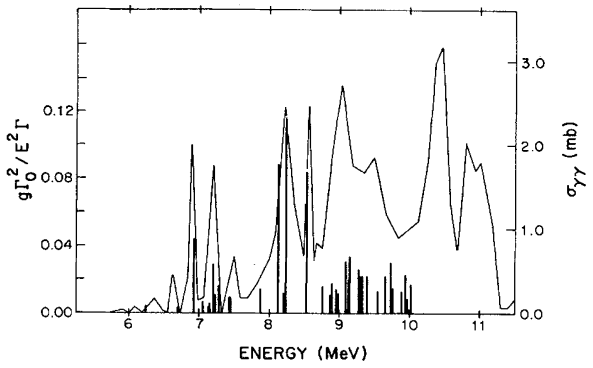

FIG. 5. Comparison of the resonance fluorescence and tagged photon results from the present work. Bars whose heights represent the values of $(1/E^2)\times(g\Gamma_0^2/\Gamma)$ for individual levels (left vertical scale) are superimposed on the low resolution average cross section data (right vertical scale). The five transitions listed in Table III and five discrete transitions below the energy range of the $\sigma_{\gamma\gamma}$ data have been omitted.

cross section $\sigma_{\gamma\gamma}(E)$ over an $E1(M1)$ resonance is related to the ground state decay width and the reduced transition probability as follows (for a thin target):

$$\int \sigma_{\gamma\gamma}(E)dE = \pi^2(\hbar c)^2 \frac{1}{E^2}\frac{g\Gamma_0^2}{\Gamma} = \frac{16\pi^3}{9(\hbar c)}\frac{\Gamma_0}{\Gamma}EB(E1,M1)\uparrow . \quad (7)$$

With a resolution of typically 100 keV, each tagged photon measurement generally reflects contributions from many discrete levels, including levels too weak to be individually distinguished above the backgrounds inherent in the resonance fluorescence measurements. On the other hand, the high resolution data provide a more detailed account of the distribution of strength among the stronger levels. Figure 5 shows a comparison of the values of $(1/E^2)\times(g\Gamma_0^2/\Gamma)$ for discrete levels with the average photon scattering cross section $\sigma_{\gamma\gamma}$ (which has not been corrected for resonant absorption).

It is clear from Fig. 5 that several of the sharp structures in the scattering cross section are related to the presence of a few very strongly excited transitions. In other cases (for example, from 9—10 MeV) there is much less correlation between the cross section peaks and the strength observed in discrete lines, reflecting the cumulative effect of the weaker transitions. A quantitative comparison of the strengths observed in the two types of measurements can be made by integrating the photon scattering cross section over each of the structures, and assuming all of the contributing transitions are dipole. A value of Γ_0^2/Γ for each peak can then be extracted, given some assumption about the extent of self-absorption in the target. The absorption correction depends on the detailed distribution of levels with large values of Γ_0, as could, for example, be determined from the high-resolution data. More simply, a range of possible values can be established using the extreme assumptions of no absorption [Eq. (7)]—appropriate when there are many weak levels—or of maximum absorption (i.e., all the strength is in one transition). The maximum absorption calculation gives an upper limit on the summed strengths of any discrete transitions within the corresponding energy interval. Although an upper limit determined in this fashion will often significantly exceed the strength of any individual level (since the data usually contain significant contributions from weak levels for which the actual absorption is much smaller than the calculation assumes), it has the advantage of being completely independent from the normalization of the high-resolution experiments. The results of this procedure are listed in Table V, and compared with the decay widths determined for discrete transitions observed in the resonance fluorescence measurements.

Two of the sharp peaks in the scattering cross section excitation function, at 6.9 and 8.5 MeV, each correspond to only one strong transition observed in the high resolution measurements. However, Table V shows that in each case only about 60% of the strength is accounted for by that discrete transition. As pointed out in Sec. III, the upper limit of $\Gamma_0^2/\Gamma = 3.40\pm0.45$ eV determined from the tagged photon measurements for the total strength in the energy interval 8.52—8.62 MeV is inconsistent with the

TABLE IV. Lorentz parameters for the giant dipole resonance in ^{56}Fe (Ref. 10).

	Line 1	Line 2
σ_0 (mb)	52	46
E_0 (MeV)	16.8	20.1
Γ (MeV)	4.33	4.09

TABLE V. Transition strength comparisons between the low- and high-resolution results for ^{56}Fe. The range of values for Γ_0^2/Γ extracted from the low resolution measurements corresponds to extreme assumptions about the absorption corrections. See the text for discussion.

Energy range (MeV)	$\int \sigma_{\gamma\gamma} dE$ (MeV mb)	Γ_0^2/Γ (eV)	Number of resolved levels	$\sum \Gamma_0^2/\Gamma$	% resolved
6.87–6.95	0.157	0.66–1.24	1	0.70	>56%
7.09–7.30	0.230	1.04–2.40	5	1.14	>48%
8.02–8.42	0.610	3.55–10.2	3	4.57	>45%
8.52–8.62	0.258	1.64–3.40	1	2.04	>60%
8.81–9.26	0.940	6.63–18.2	7	4.59	25–70%
10.31–10.51	0.616	5.82–13.2			

value of $\Gamma_0^2/\Gamma = 4.92 \pm 0.95$ eV reported by Kumagai *et al.*[11] for the level at 8.536 MeV.

In general, below 9 MeV in excitation, over half of the total bound state photon strength has clearly been resolved in the new resonance fluorescence measurements. At higher energies, although the strength is much more fragmented, a substantial fraction has nevertheless been resolved, remembering that the upper limits in Table V are greatly overestimated when the strength is shared among many levels. The present results clearly represent the most complete and detailed account of bound-state photon strength available in this mass region.

The photon scattering cross sections measured in the present experiment are believed to predominantly represent dipole strength, with significant contributions from both electric and magnetic dipole excitations. (The $E2$ strength, centered near 16 MeV according to[25] $E_x = 63A^{-1/3}$, should have only a minor effect compared with the dipole strength below 11 MeV. See Ref. 17 for the $E2$ sum rule strength and its relation to $\sigma_{\gamma T}$.) The integral of the total cross section $\sigma_{\gamma T}$ from 6 to 11.2 MeV is 8.9 MeV mb; since $\sigma_{\gamma T}$ has been extracted neglecting absorption effects, the actual integrated cross section might be somewhat ($\lesssim 50\%$) larger. If this were all $E1$ strength, it would correspond to just 1.1% of the $E1$ sum rule (836 MeV mb), comparable with the amount expected from a naive extrapolation of the giant resonance tail (see Fig. 4).

For an estimate of what fraction of the observed strength might be due to $M1$ excitations, we turn to existing calculations and experimental results for neighboring nuclei. The shell model calculations of Lipparini *et al.*,[2] covering a wide range of f-p shell nuclei, are a useful guide. [Note that the tabulated results in Ref. 2 are related to the reduced transition probabilities by

$$\Lambda_i(M1) = (4\pi/3) \times B(M1)\downarrow \ .$$

They have apparently been incorrectly equated to $(4\pi/3) \times B(M1)\uparrow$ in Refs. 4 and 26.] No calculation for ^{56}Fe was performed, but a simple interpolation between the results for ^{54}Fe (which has two fewer $p_{3/2}$ neutrons) and ^{58}Ni (with two additional $f_{7/2}$ protons) yields $\sum_i B(M1)\uparrow \approx 28\ \mu_N^2$. Two adjustments must be made to this estimate, one to reflect the fact that only $T_<$ states could be observed in the present work, and the other to account for the known quenching of $M1$ strength in this mass region.

The ratio of $M1$ strength in the isospin channels $T_<$ ($T_0 \rightarrow T_0$) and $T_>$ ($T_0 \rightarrow T_0 + 1$) can be estimated on the basis of Clebsch-Gordan coefficients. This suggests that two-thirds of the strength will be in the $T_<$ channel for ^{56}Fe; the full calculations of Ref. 2 generally show a slightly greater concentration into the $T_<$ channel than such an estimate would predict. The calculations (without quenching) would then suggest $\sum_i B(M1)\uparrow \approx 19\ \mu_N^2$ accessible to this experiment, centered somewhere in the region from 7 to 9 MeV.

However, it is well known by now that $M1$ strength in this mass region is severely quenched relative to these estimates. For example, the summed $B(M1)\uparrow$ strength found in back-angle (e,e') experiments at Darmstadt[6] for ^{50}Ti($3.4 \pm 0.4\ \mu_N^2$), ^{52}Cr($5.0 \pm 0.5\ \mu_N^2$), and ^{54}Fe($6.3 \pm 0.6\ \mu_N^2$) amounts to only 19%, 23%, and 25%, respectively, of that predicted by Lipparini *et al.*[2] Taking quenching into account, one expects $\sum_i B(M1)\uparrow \approx 3.5$–$4.5\ \mu_N^2$ in the $T_<$ channel for ^{56}Fe. This estimate can be related to an integrated cross section by rewriting Eq. (7) in terms of $\sigma_{\gamma T}$, and in the appropriate units for $M1$ transitions:

$$\int \sigma_{\gamma T} dE = 0.0443 \text{ MeV mb} \frac{EB(M1)\uparrow}{\mu_N^2} \ , \tag{8}$$

where E is in units of MeV. If all $T_<$ $M1$ strength were contained in a single excitation at 8 MeV, with $B(M1)\uparrow = 4\ \mu_N^2$ (quenched estimate), the integrated photon cross section would be 1.4 MeV mb or about 16% of the observed strength of 8.9 MeV mb. Thus one expects that perhaps 10 to 20 percent of the total photon strength observed in the present experiment would be likely to come from $M1$ excitations, with the remainder predominantly representing $E1$ strength.

No experimental evidence exists, as yet, to determine the parities of the discrete states resolved in the resonance fluorescence measurements. Kumagai *et al.*[11] suggested $M1$ assignments for all of the strong transitions they observed in ^{52}Cr and ^{56}Fe (seven in each nucleus), based in part on a comparison with the calculation of Lipparini *et al.*[2] This would mean that they had resolved 50% of the (unquenched) prediction for $T_<$ strength in ^{52}Cr and

47% in ^{56}Fe. However, the polarized photon scattering measurements of Berg *et al.*[4] at Giessen later showed that while three of the ^{52}Cr transitions are $M1$ excitations, three others are $E1$. Similarly, in ^{58}Ni several of the strongest transitions observed in photon scattering[26] are known to be $E1$. Also, the electron scattering results mentioned above show both a quenching and a fragmentation of the $M1$ strength among many levels (e.g., more than a dozen levels each in ^{52}Cr and ^{54}Fe). These observations make it extremely unlikely that all of the transitions observed in ^{56}Fe in Ref. 11 are $M1$. Even if such were the case, the amount of $M1$ strength observed would be significantly less than claimed in Ref. 11 because of the much lower values for Γ_0^2/Γ obtained in the present experiment. For the five transitions in ^{56}Fe observed in both measurements, the present work indicates that the earlier report of $M1$ strength would have to be cut in half [i.e., $\sum B(M1)\uparrow$ would be 3.9 μ_N^2 rather than 7.9 μ_N^2].

The present experiment also indirectly raises questions about the amount of $M1$ strength reported from photon scattering[4,11] on ^{52}Cr. The dominant part of the $M1$ strength [$\sum B(M1)\uparrow = 2.5 \pm 0.7\ \mu_N^2$] identified with polarized photon scattering[4] is contained in transitions first observed by Kumagai *et al.*[11] The contribution of these levels to $\sum B(M1)\uparrow$ quoted in Ref. 4 is based on the decay widths measured in Ref. 11. If the discrepancy between the widths for ^{56}Fe reported by Kumagai *et al.*[11] and those reported in the present work is the result of an error in the photon intensity calibration, then the reported widths in ^{52}Cr may also be in error (i.e., too large) by similar amounts, since the same calibration was used for both measurements in Ref. 11. Of course, other explanations are conceivable (e.g., an error in current integration) which could have affected the two sets of results differently. Nevertheless, until these absolute decay widths have been carefully remeasured, the previous results should be used with considerable caution.

Further experiments will be necessary to determine the parity change associated with the dipole transitions observed in the present work, and thus to separately map out the distributions of $E1$ and $M1$ strength in ^{56}Fe. Our measurements are complementary in several important respects to the standard techniques for measuring parity changes. For example, the beautiful bremsstrahlung $(\vec{\gamma},\vec{\gamma}')$ system at Giessen[4,27] lacks the sensitivity of the present work, due to the use of a low duty-cycle accelerator and the difficulty of generating a polarized beam. High sensitivity in bremsstrahlung experiments is critical for avoidance of systematic errors in extracting widths, even for the strong transitions. Since the Ge(Li) escape peaks for an 8 MeV transition can be much larger than the full energy peak, significant errors can be produced by weak transitions lying 511 or 1022 keV above the transition of interest. Runs with varying end point energies (to reduce backgrounds for transitions of interest, to distinguish elastic from inelastic scattering, and to guard against feeding from higher lying levels) are also important in extracting reliable decay widths. These tasks are much more easily performed with high duty-cycle unpolarized beams, and provide information important for the interpretation of the necessarily more difficult measurements with polarized beams. The photon scattering measurements are also complementary to back-angle (e,e') scattering because they are an independent source of (model-independent) transition strengths ($g\Gamma_0^2/\Gamma$), with a significantly higher resolution (typically $\sim$7 keV vs $\sim$30 keV in Ref. 6), and are insensitive to the major source of possible confusion (the dense background of $M2$ transitions) in the electron measurements. Hopefully the present work can form the foundation for a detailed understanding of the $M1$ and $E1$ strength distributions in ^{56}Fe. Preliminary accounts of portions of the present work appeared in Refs. 28 and 29, which are superseded by the present report.

ACKNOWLEDGEMENTS

The authors would like to acknowledge the constant support and encouragement of their late friend and colleague Peter Axel, who provided the original motivation for this work. We wish to thank Lloyd Young and the accelerator staff for their assistance in providing reliable electron beams. This research, including the development and operation of MUSL-2 and its experimental areas, was supported by a grant from the U.S. National Science Foundation.

---

*Present address: Physics Department, University of Pennsylvania, Philadelphia, PA 19104.

†Present address: Laboratory for Astronomy & Solar Physics, NASA/Goddard Space Flight Center, Greenbelt, MD 20771.

‡Present address: AT&T Bell Laboratories, Crawford Hill Laboratory, Box 400, Holmdel, NJ 07733.

[1]Mitsuaki Obu and Tokuo Terasawa, Prog. Theor. Phys. **43**, 1231 (1970).

[2]E. Lipparini, S. Stringari, M. Traini, and R. Leonardi, Nuovo Cimento **31A**, 207 (1976).

[3]H. E. Jackson and E. N. Strait, Phys. Rev. Lett. **27**, 1654 (1971).

[4]U. E. P. Berg *et al.*, Phys. Lett. **103B**, 301 (1981).

[5]R. A. Lindgren *et al.*, Phys. Rev. C **14**, 1789 (1976).

[6]G. Eulenberg *et al.*, Phys. Lett. **116B**, 113 (1982).

[7]J. Rapaport *et al.*, Phys. Lett. **119B**, 61 (1982).

[8]A. Härting, W. Weise, H. Toki, and A. Richter, Phys. Lett. **104B**, 261 (1981).

[9]C. Ngo-Trong, T. Suzuki, and D. J. Rowe, Nucl. Phys. **A313**, 15 (1979).

[10]T. J. Bowles *et al.*, Phys. Rev. C **24**, 1940 (1981).

[11]N. Kumagai, T. Ishimatsu, E. Tanaka, K. Kageyama, and G. Isoyama, Nucl. Phys. **A329**, 205 (1979).

[12]Ph. B. Smith and W. Segeth, Nucl. Phys. **A398**, 397 (1983).

[13]P. Axel *et al.*, IEEE Trans. Nucl. Sci. **NS-24**, 1133 (1977).
[14]T. Chapuran, R. Vodhanel, and M. K. Brussel, Phys. Rev. C **22**, 1420 (1980).
[15]J. T. Routti and S. G. Prussin, Nucl. Instrum. Methods **72**, 125 (1969).
[16]P. Axel *et al.*, IEEE Trans. Nucl. Sci. **NS-22**, 1176 (1975).
[17]R. M. Laszewski and P. Axel, Phys. Rev. C **19**, 342 (1979).
[18]G. A. Bartholomew *et al.*, Nucl. Data Tables **A3**, 367 (1967).
[19]R. L. Auble, Nucl. Data Sheets **20**, 253 (1977).
[20]H. Verheul and R. L. Auble, Nucl. Data Sheets **23**, 455 (1978).
[21]J. Lachkar, J. Sigaud, Y. Patin, and G. Haouat, Nucl. Phys. **A222**, 333 (1974).
[22]F. R. Metzger, *Progress in Nuclear Physics* (Pergamon, New York, 1959), Vol. 7, p. 53.
[23]Michael Danos and Walter Greiner, Phys. Rev. **134**, B284 (1964).
[24]W. Biesiot and Ph. B. Smith, Phys. Rev. C **24**, 808 (1981).
[25]F. Bertrand, Annu. Rev. Nucl. Sci. **26**, 457 (1976).
[26]K. Ackermann, K. Bangert, U. E. P. Berg, G. Junghans, R. K. M. Schneider, R. Stock, and K. Wienhard, Nucl. Phys. **A372**, 1 (1981).
[27]R. K. M. Schneider, Diploma thesis, Universität Giessen (unpublished).
[28]R. Starr, P. Axel, and L. S. Cardman, Bull. Am. Phys. Soc. **22**, 1021 (1977).
[29]T. Chapuran, R. Vodhanel, and M. K. Brussel, Bull. Am. Phys. Soc. **23**, 507 (1978).